

THERMAL ANALYSIS OF HIGH EXPLOSIVES:
LIQUID STATE DECOMPOSITION OF RDX

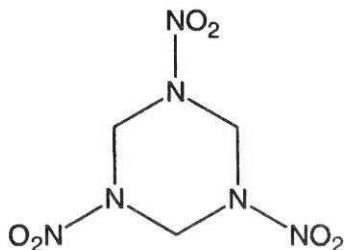
G. T. Long (long@chemistry.utah.edu), S. Vyazovkin, B. A. Brems and C. A. Wight
Center for Thermal Analysis, Department of Chemistry, University of Utah
315 S. 1400 E., Salt Lake City, UT 84112-0850

ABSTRACT

Nonisothermal thermogravimetric analysis (TGA) and differential scanning calorimetry (DSC) have been applied to the thermal decomposition of RDX. Model-free isoconversional analysis of TGA and DSC traces show that RDX primarily evaporates in an open pan with an activation energy of $E_{\alpha} \sim 100 \text{ kJ mol}^{-1}$. Similar analysis of pierced pan TGA and DSC and closed pan DSC curves reveal that RDX decomposes in the liquid state under these conditions with $E_{\alpha} \sim 150 - 195 \text{ kJ mol}^{-1}$. An increasing plot of the integrated and normalized exotherm versus heating rate, β , in pierced pan DSC experiments indicates that decomposition has a higher activation energy than that for evaporation and becomes more important relative to evaporation as a function of the extent of conversion, α . In a closed pan, RDX generates a constant heat release of $\sim 500 \text{ kJ mol}^{-1}$ that is independent of both β and mass. These results suggest that the bubbles formed in the fizz zone of burning RDX consist of gaseous reaction products of liquid RDX decomposition rather than intact gas phase RDX molecules.

INTRODUCTION

Hexahydro-1,3,5-trinitro-1,3,5-triazine (RDX) is the most prevalent



explosive in plastic explosives and has found widespread commercial and military use. An important aspect of its characterization is the determination of the kinetics and energetics and the mechanism of its slow cook off chemistry (1-3). Isoconversional kinetic analysis has been applied to TGA and DSC traces that measure the kinetics of RDX cook off chemistry. This model-free method of analysis can detect multistep kinetics characteristic of solid state processes and also determines activation energies as a function of the

extent of conversion (4-5). Such information can lead to the safer manufacture, handling and storage of high energy materials including explosives such as RDX.

EXPERIMENTAL

RDX, obtained from the Army Research Laboratories, Aberdeen Proving Ground, MD, was studied as a granular powder.

TGA experiments were performed on a Mettler-Toledo TGA/STDA851^o module in the nonisothermal heating mode. $\sim 1.0 \text{ mg}$ RDX samples were studied in $40 \mu\text{L}$ pans in open pan and pierced pan (1.0 mm piercer) experiments; they were conducted at heating rates of $\beta = 7.5 - 20 \text{ }^{\circ}\text{C min}^{-1}$ over a temperature range of $25 - 300 \text{ }^{\circ}\text{C}$ using N_2 as the purge gas at a flow rate of $70 \mu\text{L min}^{-1}$.

DSC experiments employed a Mettler-Toledo DSC821^o module using the nonisothermal heating mode. $40 \mu\text{L}$ pans were used in open, pierced and closed pan experiments using N_2 as the purge gas at a flow rate of $80 \mu\text{L min}^{-1}$. All DSC experiments were conducted over a temperature range of $25 - 300 \text{ }^{\circ}\text{C}$ for $\beta = 2.5 - 20.0 \text{ }^{\circ}\text{C min}^{-1}$. RDX samples sizes in DSC experiments were: open pan, $\sim 1.0 \text{ mg}$; pierced pan (1.0 mm piercer), $\sim 0.5 \text{ mg}$; closed pan, $20 - 80 \mu\text{g}$.

Error limits shown in E_{α} versus α plots represent 95% confidence limits.

RESULTS

Thermogravimetric Analysis. The mass loss in nonisothermal TGA traces for open pan samples of RDX occurs in two stages (Figure 1a) and approaches 100% of the initial mass. The first and main stage of mass loss occurs between $170 - 260 \text{ }^{\circ}\text{C}$. The second, much shallower stage takes place between $240 - 290 \text{ }^{\circ}\text{C}$. Isoconversional analysis of the traces in Figure 1a yields constant activation energies of $\sim 99 \text{ kJ mol}^{-1}$ for $0.02 \leq \alpha < 0.60$ that apply to the first stage of mass loss (Figure 1b).

Nonisothermal TGA curves for pierced pan samples of RDX show a single stage of mass loss that exceeds 95% of the initial mass and that occurs over a range of $210 - 270 \text{ }^{\circ}\text{C}$ (Figure 2a). Applying isoconversional analysis to the traces in Figure 2a gives an E_{α} vs. α plot that decreases from $E_{\alpha} = 235 \text{ kJ mol}^{-1}$ at $\alpha = 0.02$, plateaus at E_{α}

$\sim 195 \text{ kJ mol}^{-1}$ for $0.06 < \alpha < 0.50$, and finally decreases to $E_a = 127 \text{ kJ mol}^{-1}$ at $\alpha = 0.98$ (Figure 2b).

Differential Scanning Calorimetry. Isoconversional analysis of the exotherm in nonisothermal DSC traces of open pan samples of RDX gives a relatively constant value of $E_a \sim 102 \text{ kJ mol}^{-1}$ for $0.20 < \alpha < 0.98$ (not shown). Similar analysis of the exotherm in DSC traces of pierced pan samples yield activation energies that show a slow sigmoidal decrease from $E_a = 161 \text{ kJ mol}^{-1}$ at $\alpha = 0.02$ to $E_a = 133 \text{ kJ mol}^{-1}$ at $\alpha = 0.98$ (not shown). The size of the exotherm increases relative to the sharp structured endotherm that precedes it upon going from an open pan to a pierced pan to a closed pan sample; such a DSC curve for a closed pan sample is shown in Figure 3a. Isoconversional analysis of DSC traces of closed pan samples leads to an E_a vs. α plot that sigmoidally decreases from $E_a = 205 \text{ kJ mol}^{-1}$ at $\alpha = 0.02$ to $E_a = 136 \text{ kJ mol}^{-1}$ at $\alpha = 0.98$ (Figure 3b).

The heat flow in pierced pan experiments was plotted as function of β and in closed pan experiments as a function of β and of mass. Figure 4a shows that the heat flow vs. β increases in a pierced pan for $\beta \leq 12.5 \text{ }^\circ\text{C min}^{-1}$; above this heating rate, the heat flow reaches an asymptotic value of $\sim 1750 \text{ J g}^{-1}$. A relatively constant heat release of $\sim 2250 \text{ J g}^{-1}$ occurs in for closed pan samples that is independent of β and of mass.

DISCUSSION

This thermal analysis study of RDX by TGA and DSC shows a competition between endothermic vaporization in an open pan and exothermic decomposition in the increasingly confined environments of pierced pan and closed pan samples.

Thermogravimetric Analysis. The activation energies of $E_a \sim 99 \text{ kJ mol}^{-1}$ determined for the first and major stage of mass loss in open pan experiments (Figure 1) are in good agreement with a literature value for vaporization of RDX of 94.4 kJ mol^{-1} (6). As the onset of the mass loss occurs below the melting point of RDX, $204 \text{ }^\circ\text{C}$ (6), some sublimation may also occur. The mass loss in pierced pan TGA experiments (Figure 2a) occurs in one stage and shifts to a higher temperature range than in open pan experiments. Moreover, the mass loss is more temperature sensitive and corresponds to a higher activation energy of $E_a \sim 195 \text{ kJ mol}^{-1}$ (Figure 2b) showing that a different process dominates in pierced pan experiments than in open pan experiments. As the onset of mass loss in pierced pan samples occurs above the melting point of RDX, this process is attributed to liquid state decomposition of RDX.

Differential Scanning Calorimetry. A relatively constant activation energy of $E_a \sim 102 \text{ kJ mol}^{-1}$ determined by isoconversional analysis of open pan experiments is very similar to that determined in open pan TGA experiments and further supports vaporization of RDX in an open pan. Comparing the results of open

pan, pierced pan, and closed pan DSC experiments that are increasingly confined, show systematic trends. First, all three environments show a structured melting endotherm that peaks at $204 \text{ }^\circ\text{C}$, followed by an exotherm. Second, the size of the exotherm relative to the endotherm increases with increasing confinement. Third, the activation energies determined by analyzing the exotherms increase with increasing confinement. This difference in activation energies shows that two different processes are in competition. Further evidence of this competition is an increasing heat release as a function of β determined in pierced pan experiments (Figure 4a). The positive slope at the beginning of this plot shows that the process that dominates at higher heating rates, exothermic decomposition, has a higher activation energy than that which dominates at lower heating rates, vaporization.

A closed pan sample generates a constant heating release of $\sim 2250 \text{ J g}^{-1}$ (Figure 4) ($\sim 500 \text{ kJ mol}^{-1}$) as both a function of heating rate and of mass. Twenty percent of this value corresponds to the heat needed to offset that taken up by vaporization and to account for the small exotherm observed in open pan experiments.

The results of this thermal analysis study of RDX suggest that at the high temperatures and heating rates of combustion conditions, exothermic decomposition will be strongly favored relative to vaporization. Hence, the bubbles observed in the fizz zone of burning RDX are comprised of gaseous reaction products of liquid state RDX decomposition and not of intact RDX molecules.

CONCLUSIONS

A competition occurs between evaporation and exothermic decomposition of RDX in nonisothermal TGA and DSC experiments. Isoconversional analysis of open pan TGA and DSC experiments give activation energies of $\sim 100 \text{ kJ mol}^{-1}$, consistent with a literature value for RDX evaporation. A shift in the mass loss to higher temperatures in pierced pan TGA experiments relative to those in open pans shows that different processes dominate in each environment. Applying isoconversional analysis to the mass loss in pierced pan TGA experiments and to the exotherms above the melting point in pierced pan and closed pan DSC experiments show that decomposition of RDX occurs in the liquid phase in these environments with an activation energy of $\sim 150 - 195 \text{ kJ mol}^{-1}$. An increasing heat flow in pierced pan DSC experiments also shows that exothermic decomposition has a higher activation energy than vaporization. The exotherms in closed pan DSC experiments correspond to a constant heat release of $\sim 500 \text{ kJ mol}^{-1}$ that is independent of β and of mass. These results suggest that the bubbles observed in burning RDX under combustion conditions likely consist of gas phase reaction products rather than intact RDX molecules.

ACKNOWLEDGEMENTS

We gratefully acknowledge ONR (MURI contract No. N00014-95-1-1339) and C-SAFE (LLL subcontract B341493) for supporting this work. We also thank the Mettler-Toledo Corporation for the generous donation of the TGA and DSC instruments used in this work.

REFERENCES

1. Schroeder, M. A. Proceedings of the 21st JANNAF Combustion Meeting, Oct. 1984, CPIA Pub. No. 412, Vol. II, p 595.

- Schroeder, M. A. Proceedings of the 23rd JANNAF Combustion Meeting, Oct. 1986, CPIA Pub. No. 457, Vol. II, p 43.
- Adams, G. F.; Shaw Jr., R. W. *Annu. Rev. Phys. Chem.* **1992**, *43*, 311.
- Vyazovkin, S.; Wight, C. A. *Annu. Rev. Phys. Chem.* **1997**, *48*, 125.
- Vyazovkin, S.; Wight, C. A. *J. Phys. Chem. A* **1997**, *101*, 8279.
- Hoffman, H. J. CPIA/M3 Report, August 1981.

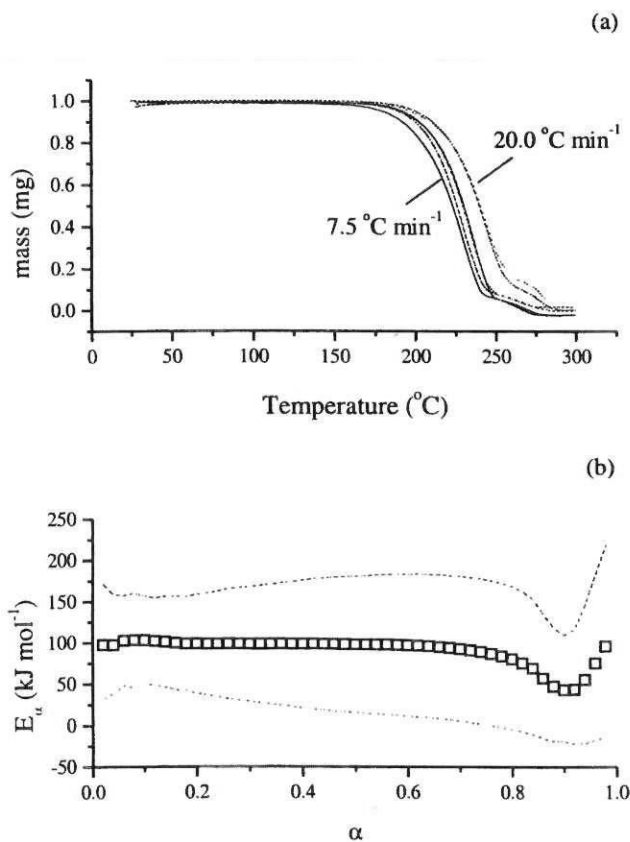


Figure 1. (a) Nonisothermal TGA traces of open pan samples of RDX for heating rates of $\beta = 7.5, 10.0, 12.5, 15.0, 17.5, 20.0^\circ\text{C min}^{-1}$. (b) A plot of activation energy versus α resulting from the application of isoconversional analysis of the curves in (a).

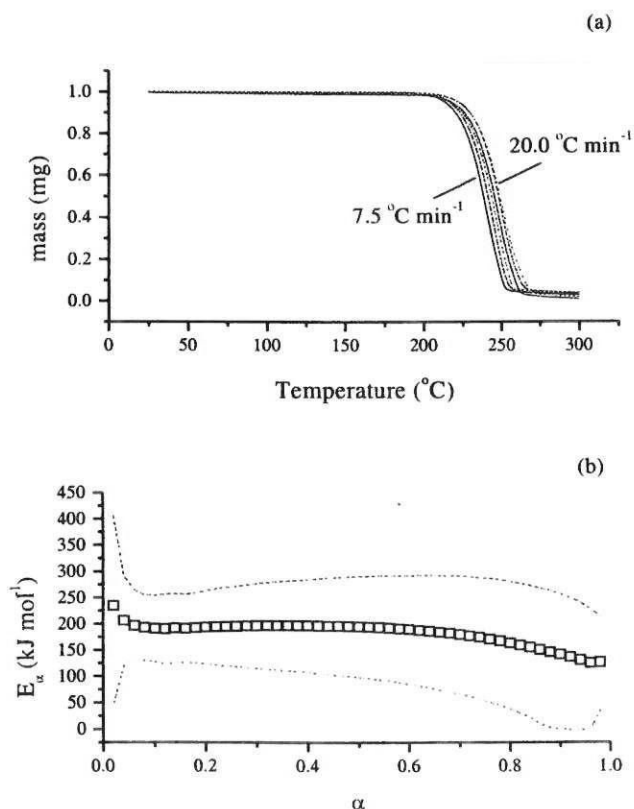


Figure 2. (a) Nonisothermal TGA curves collected in pierced pans for samples of RDX for heating rates of $\beta = 7.5, 10.0, 12.5, 15.0, 17.5, 20.0^\circ\text{C min}^{-1}$. (b) Plot of activation energy versus α by applying isoconversional analysis of the curves in (a).

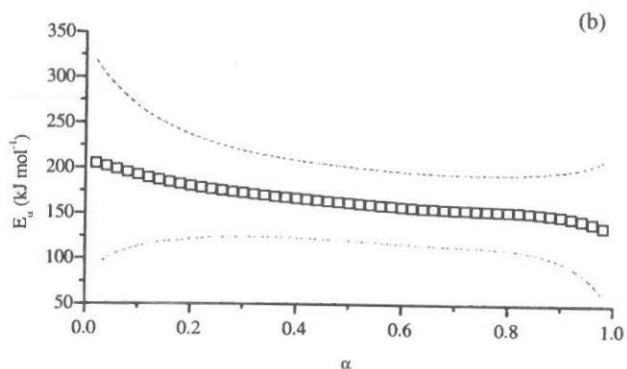
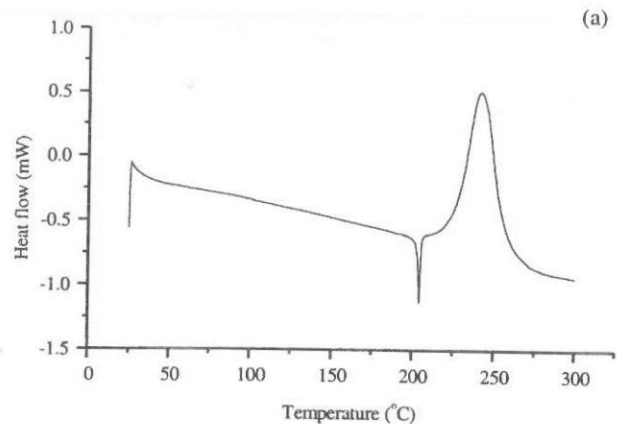


Figure 3. (a) Nonisothermal DSC trace of a closed pan sample of RDX collected at $\beta = 10.0^\circ\text{C min}^{-1}$. (b) A plot of activation energy as a function of α as determined by isoconversional analysis of traces such as those in (a) for $\beta = 2.5, 5.0, 7.5, 10.0, 12.5, 15.0, 17.5, 20.0^\circ\text{C min}^{-1}$.

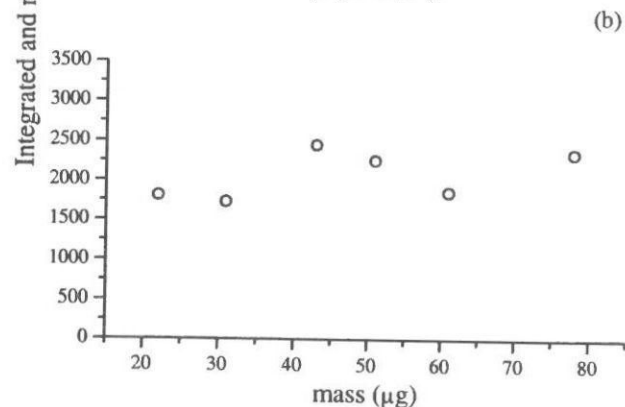
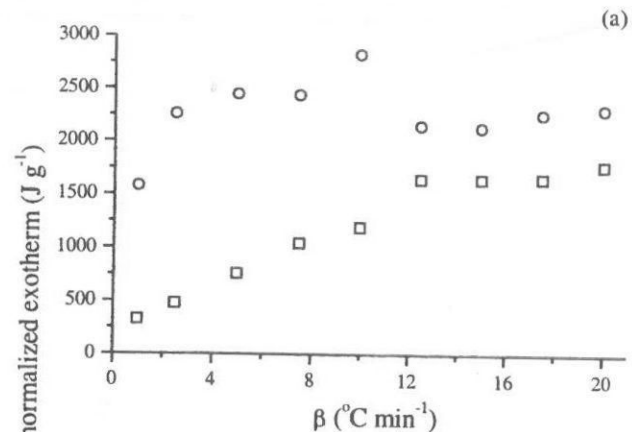


Figure 4. (a) The integrated and normalized heat flow as a function of β for pierced pan (\square) and closed pan (\circ) samples of RDX. (b) Integrated and normalized heat release versus mass in closed pan samples.